Report: Convalescent Blood Treatment for COVID-19: Are Local Donors Enough?

Pamela K Douglas, PhD [1,2] , Farzad V. Farahani, PhD [2], David B. Douglas[1], M.D., M.P.H.,[3] Susan Bookheimer, PhD [1]

1.) Department of Psychiatry and Biobehavioral Medicine, David Geffen School of Medicine, UCLA
2.) Modeling, Simulation and Computer Science, UCF
3.) Harvard T.H. Chan School of Public Health

Abstract: COVID-19 is now a global pandemic, and an effective vaccine may be many months away. Over 100 years ago, Spanish flu fatalities were attenuated when doctors began treating patients with blood plasma donated by recovered (or convalesced) survivors. Passive immunity transfer via administration of convalesced blood product (CBP) appears to represent a readily available and promising avenue for mitigating mortalities, expediting recovery time, and even prophylaxis against the SARS-CoV-2 virus. Here, we review challenges to CBP efficacy, and present a graph theoretical model of transmission dynamics that identifies evolving "hubs" of COVID-19 cases. Importantly, this model suggests that CBP efficacy may rest on an efficient and distributed global sampling scheme as opposed to CBP pooled from local donors alone.

Key words: COVID-19; convalescent plasma, graph theory, antigenic shift, SARS-Cov-2, IVIG

Introduction

Transferring immunity from a recovered host to a newly infected patient is not novel. In 1890, serum extracted from animal hosts was used to treat children with diphtheria in one of the first noteworthy immunotherapy successes (*1*). Prior to the age of antibiotics, antibody transfer from a recovered survivor to a newly infected recipient was widely used to treat human infectious diseases, and by the 1930s, over 80% of patients with type1 pneumonia admitted to a Boston hospital were treated with type-specific serum (*2*). Although serotherapy was mostly applied during bacterial infections, viruses such as measles, mumps, varicella zoster, and poliomyelitis were treated with convalesced blood product (CBP).

Recently, the SARS-Cov-2 virus has caused a global pandemic of alarming morbidity and mortality. Common symptoms of COVID-19 resemble that of the severe acute respiratory syndrome (SARS) including fever, dry cough, difficulty breathing (dyspnoea), and fatigue (*3*). For approximately half of patients, the clinical course is uncomplicated with no abnormalities on chest radiographs (*4*)(*5*). However, as the disease progresses, ground-glass opacities are reported on the majority of chest computerized-tomography images and ~6% of cases require mechanical ventilation (*5*). In many cases, the progression of the disease along with the radiographic findings appear to wax and wane (Figure 1A).

Social distancing and public health measures ultimately put an end to the SARS outbreak of 2002, which caused 774 fatalities (*6*) and an estimated $100 billion to the global economy (*7*). The SARS-Cov-2 pandemic, now orders of magnitude larger, will undoubtedly cause catastrophic economic burden, and the prolonged social distancing measures are expected to have a major impact on mental health (*8*). Unfortunately, there are currently no effective medications, vaccines or treatments for SARS-Cov-2, and there is an urgent need to identify target drugs and minimize the translational gap between preclinical testing and treatment (*9*). Ultimately, an effective vaccine may be many months away.

In contrast, the historic practice of CBP administration represents a readily available therapeutic avenue for SARS-Cov-2. Recent studies with other beta coronaviruses suggest that patients who received CBP had improved clinical outcomes for middle east respiratory syndrome (MERS) and SARS (*10*), though recent meta-analyses suggest mixed results (*12*)(*13*). Early reports suggest a clinical benefit for CBP in rescuing COVID-19 patients, albeit on small sample sizes (*11*).

Overall, the long history of antibody therapeutics has provided insight into the some of the fundaments that subserve and are required for its efficacy. Challenges to successful CBP therapy include unknown dose requirements, donor batch variability, mixed immunity transfer, serological and molecular diagnostic false positives, variable seroconversion rates, and timely distribution of strain-specific antibodies in the event the virus evolves. Here, we review these key challenges and suggest a graph theoretic epidemiological model for predicting evolving needs and distributed strategies for CBP donor sampling.

Convalescent Blood Therapeutics: Challenges with Preparation

Convalescent blood products (CBP) can be used to achieve passive or artificially acquired immunity against infectious diseases, where neutralization is thought to be the primary mechanism of protection against viral infections (*14*). In the pre-antibiotic era, whole blood, plasma or serum were often derived from a single surviving host that had acquired active or humoral immunity to the infection.

In recent years, immunoglobulin (Ig) for intravenous or intramuscular administration, high-titre human Ig, and polyclonal or monoclonal antibodies have become more common (*15*). Intravenous immunoglobulin (IVIG) is now typically prepared from the pooled plasma of thousands of donors containing primarily IgG, and only trace amounts of either IgM or IgA (*16*), the latter of which can induce anaphylactic reactions in patients with IgA deficiency. In recent decades, IVIG has become the gold standard treatment for an expanding number of autoimmune diseases, given its broad repertoire of neutralizing antibodies across a range of pathogens (*17*).

Convalescent plasma therapy is generally considered safe (*18*). However, there are known adverse effects which should be considered in light of the patient's specific risks for side effects in combination with disease mortality. Immediate and mild adverse reactions include general malaise or serum sickness. Rare and delayed side effects are more severe including renal failure, thromboembolic events, neurological toxicity, and pulmonary complications (*19*). The risks of transmitting infections from donor to recipient (e.g., HIV) or from donor to a transfusion service personnel (e.g., COVID-19) also cannot be eliminated. Lastly, the half-life of IgG is approximately 3-4 weeks, thus treatments are required every few weeks (*17*).

Unfortunately, there are significant challenges when producing IVIG for distribution. Variability in the donor population, number of donors, and purification methods induces heterogeneity in the preparation (*20*). If plasma is taken from a (small) random sample of serologically positive donors, then there is a certain probability that the batch will be SARS-Cov-2 antibody poor. Methods for identifying donors rests on a combination of molecular and serological diagnostics. Unfortunately, both are unlikely to be positive simultaneously (Figure 1b).

Timing (and Testing) is everything

Ideally, both the viral strain and the immune response temporal profile would be well characterized for all CBP donors and recipients. Acquiring this knowledge requires a minimum of two tests. First, a molecular diagnostic test would identify the viral strain, typically via a polymerase chain reaction (PCR) test operating on a nasopharyngeal or similar swab in combination with specifically designed primers or probes. Secondly, a serological test would identify the presence of SARS-Cov-2 specific antibodies, most commonly with the use an enzyme-linked immunosorbent assay (ELISA) serological test.

Simultaneous administration of these two tests is unlikely to reveal both unknowns. PCR tests are typically positive during viral shedding, detected in the early stages of the disease. Daily

real-time PCR (RT-PCR) tests on COVID-19 patients revealed that these tests were positive for a median of 12 days (range 1-24) (*4*). Antibodies are also typically produced in a unique temporal pattern across individuals in response to infection, as is the case with SARS-Cov-2. Preparing an ideal IVIG batch would require donation when there is a strong presence of IgG antibodies, and therefore delaying donations until IgM antibodies have subsided. In one patient reported, the IgM levels took at least 18 days to subside (*3*) (Figure 1B).

It is also possible for the donor to test positive on the PCR test, yet negative on the serological test. This might occur in the case of a PCR false positive, a serological false negative, or simply the case where the donor had a mild case and therefore produced very few antibodies which would subsequently be useful for CBP therapy. In this case, the donor would be SARS-Cov-2 antibody poor.

Conversely, a potential donor may receive a false negative on a PCR test, which could be detrimental in the event that there is a scarcity of donors (Perez-Cameo 2020). The majority of PCR primers are based on the Spike protein sequence as indexed with the original Wuhan strain (*21*). Given that there are multiple co-circulating genotypes of SARS-Cov-2 (discussed below), it is possible that a primer may not anneal appropriately on an alternate strain.

Timing of antibody receipt is also essential. Studies during the SARS outbreak suggest that CBP infusion is most effective when the patient is both PCR positive and seronegative for the virus (*10*). CBP therapy is generally most efficacious during the earliest stages of infection, and prior to production of a patients own immune response (*2*) (Figure 1C). The utility of CBP for COVID-19 prophylaxis is unknown, but warrants further exploration.

Evolutionary Transitions and Cross-Neutralization

SARS-Cov-2 is a new founder beta coronavirus which consists of a single strand of positive sense RNA (*22*), and is the seventh coronavirus known to cross the species barrier into humans (*23*). Phylogenetic analyses suggest a zoonotic origin (animal etiology) due to its homology with SARS-like coronavirus found in bats (*3*), a natural reservoir for genetic variability of these viruses (*24*). Considerable evidence from next generation and PCR sequencing now points to multiple co-circulating genotypes of SARS-Cov-2 (*25*);(*26*); (*27*). In one study, at least 13 variation sites were identified, with at least two in open reading frames having mutation rates of up to 30% (*21*).

Antigenic drift typically results in mutations that have no discernible effect on clinical presentation. For example, the D614G mutation due to antigenic drift has little effect on the rate of SARS-Cov-2 hospitalizations. However, the G614 form quickly became the predominant strain around the globe forming its own “G-clade” haplotype (*26*). It is unknown if this increased prevalence was due to increased fitness or simply by random chance.

Genetic reassortment amongst circulating strains is also an important factor in the evolutionary trajectory of coronaviruses (*28*); (*24*). In order for reassortment to occur, two distinct parent strains must co-infect a host. There is already evidence for genetic recombination in SARS-Cov-

2, with the emergence of the S9423P mutation identified across a variety of geographic locations in Belgium. The precise mechanism subtending the increased fitness of the G614 mechanism is unknown. However, one immunological hypothesis suggests that this form may mediate antibody escape, making a host susceptible to subsequent infections (*26*).

Fortunately, viral progeny are often less pathogenic. After all, a virus that rapidly kills its host is less likely infect another host successfully. For example, the ancestral 1918 influenza A viral lineage still circulates today in a much more attenuated form (*29*). Nonetheless, the ability to evade or alter immune response is an important factor of increased viral fitness.

Importantly, it is unclear if immunity to one strand will effectively cross-neutralize an altered target. Some evidence from the early SARS-Cov-2 strain suggested some cross-reactivity with horse serum (*3*). However, the SARS-Cov virus shares ~79% homology with SARS-Cov-2, yet a number of tested monoclonal antibodies specific to receptor biding domains in SARS-Cov had low affinity for SARS-Cov-2, suggesting minimal antibody cross-neutralization (*30*).

Predicting viral phenotypic properties from genetic sequences that have undergone antigenic drift and recombination remains very challenging. Appreciating the prevalence of viral strains within geographic clusters and their associated networks may help model evolutionary trajectories and identify regions for increased viral surveillance and donor/sampling for CBP. The efficacy of CBP therapy may rely on identifying causal factors that lead to genetic shifts of immunological import - particularly given the short time window for which it must be administered.

Small World Transmission Dynamics

Complex systems, such as the epidemiology of SARS-Cov-2, can be described mathematically with the use of a graph. Complex network analysis, rooted in classical graph theory, has been used successfully to characterize statistical dependencies in large scale data ranging from social networks (*31*) to functional connections in the brain (*32*). Importantly, structural or position data (nodes) can be explicitly defined along with their pairwise functional relationships (edges) on the same map, thus revealing topological correspondences between geographic structure and function (*33*).

Here, we applied complex network analysis to the spread of COVID-19 throughout the US, whereby each state was considered as a node and the magnitude of case report temporal correlations are reflected in the links or edges (Figure 2). This analysis is useful for classifying nodes into local cliques (modules), identifying hubs, as well as quantifying global properties of the network. Interestingly, Washington State, where the initial case reports in the US occurred was never a highly connected or centralized hub, as revealed by the inner circle weights on connectograms (Figure 2c). For additional results comparing relative and cumulative cases, please see Supplementary Results. New York was clearly a node with high degree (densely connected) that not only participates in the northeast modular structure, but also provides links with other cliques, and is

therefore was important connector hub during the early spread of the disease. In contrast, Maine has maintained a low degree of edges throughout the spread of the pandemic.

Appreciating hubs can be useful for public health planning, predicting CBP need, and appropriate distribution of critical care supplies. Geographically isolated regions with low degree and sparse connectivity (e.g., Maine) may also play an important role in shaping the genetic landscape. Ecology, climate, and geographic distribution of viral strains help shape the tempo of viral evolution, and mutation hot spots are often surrounded by cold spots (*34*)(*35*). The determinants of evolutionary rate variability for SARS-Cov-2 and the mosaic of reciprocal gene-host-environmental effects on fitness and the possibility of allopatric effects on strain diversity require further study. Geographically isolated communities can have strains that drift separately from more connected subpopulations. To ensure a CBP pool that represents the broad repertoire of immunity, it may be advantageous to recruit blood donors from these regions as well.

Small-worldness is a property of some networks whereby most nodes are not neighbors, but they can be reached in a small number of steps from all other nodes with a small average path length. In this sense, small world networks represent a tradeoff between organized networks and those with random connectivity. Interestingly, as the COVID-19 pandemic spread throughout the US, the network became increasingly small world. The implications of a small world COVID-19 epidemiological network topology on CBP therapy is that local donations alone are expected to fail in providing the diversity of immunity necessary for effective immunity transfer.

Conclusions

Convalescent blood products containing antibodies have been used for over a century in the setting of pandemics. Although CBP usage declined after the introduction of antibiotics, it has continued to serve a crucial role in a number of outbreaks of viral etiology from West Nile virus to Ebola (*14*). During its therapeutic tenure, it has become clear that plasma from a single donor will not suffice. Intravenously administered antibodies, pooled from thousands of donors, is now considered the gold standard treatment for a variety of autoimmune conditions. Furthermore, our graph theoretic results strongly suggest that not only will a single donor not suffice, but pooling blood from a single donor site or hospital is not expected to be sufficient either.

At the onset of any pandemic, there are expected to be many more patients with active infections than those who have recovered. Randomized serological screening has provided evidence for the existence of asymptomatic infections, and immune response in paucisymtomatic individuals (*18*). Therefore, serological assays may be useful in identifying additional donors at the onset of a pandemic, in the event of a significant mutation of an existing virus, or in conditions of donor scarcity. Although the duration of immunity to a

particular strain of SARS-Cov-2 is unknown, there are examples of humans maintaining seroreactivity to the 1918 influenza nearly 90 years after exposure (*36*). Longitudinal studies of seroreactivity in convalesced COVID-19 patients are clearly needed to help inform CBP sampling strategies and appreciate the probability of reinfection.

Serological assays alone will not provide the information necessary to understand how the clinical course of the disease and temporal profile of the immune response may differ across different viral strains and ecological factors. RNA viruses, in general, have a highly variable rate of evolution. In one report, at least six different clades of SARS-Cov-2, distributed throughout the extant phylogenetic tree, were identified in different boroughs of New York (*37*). Major hubs for the pandemic are expected to have considerable genetic flow into and out of the region. In this sense, sampling CBP from this densely connected hubs will likely provide immunity to a diversity of strains, but not to all strains.

In our complex network analysis here, we identified cliques or modules as well as major connector hubs with high betweenness centrality. This analysis also identified regions with very sparse connectivity with other regions in the US. Our analysis was consistent with open source phylogenetic reports from NextStrain, suggesting that Washington state was never an early hub for COVID-19 spread throughout the US. Given that the warmer seasonal weather failed to abate the disease, there has been more time for the perseveration of antigenic drift than for typical viruses. It is possible that geographically isolated regions with reduced flow or connectivity may be more prone to diverging effects. These regions (e.g., Maine) should therefore be the target of sero-surveillance and molecular genetics testing programs until more is known about the environmental effect on natural selection and the trajectory of viral evolution.

Thus far, a number of mathematical modeling tools have been developed to examine various aspects of SARS-Cov-2, including its phylogeography, and latent variable dynamics. However, there is a critical need to integrate multimodal data across levels of abstraction within the context of predictive modeling (*38*), and to contextualize these findings for the purpose of effective CBP therapeutics.

The small world network topology of SARS-Cov-2 spread suggests that enrolling donors via local programs alone is unlikely to provide a broad repertoire of immunity for effective treatment and potentially prophylaxis of COVID-19. With an increasingly itinerant society and small world epidemiological network properties, a coordinated global effort is crucial if the old CBP treatment is to be revived for novel therapeutic purposes.

Figures:

Figure 1: (a) A 67 year old female COVID-19 case. From left to right: Baseline chest x-ray from 2014, initial presentation of COVID-19 4/13/20 showing bilateral areas of patchy airspace and along the lung periphery; 3 days later showing slight improvement of disease; CT scan 3 days later on 4/19/20 showing diffuse ground glass opacity corresponding to airspace disease on chest xray; the following day, chest x-ray shows mild improvement; on 4/21/20 the disease worsened showing the overall waxing and waning of opacity in radiological findings. (b) Serially collected polymerase chain reaction (PCR) data overlaid with serological assays collected serially; data reproduced from Zhou et al. 2020 & (*39*)Pan et al. 2020 (c) Flow diagrams illustrating convalescent blood product (CBP) treatment and donor pooling scenarios. (Upper left) the healthy individual is infected, and either acquires active immunity, a weak immune response, or the disease results in fatality. (Middle left) The infected individual is treated with CBP in a timely manner and acquires passive immunity. (Lower Left) The individual is treated with CBP, yet the administration takes place after the individual's immune response has initiated, and is therefore ineffective at conferring passive immunity. (Upper Right) Pooling CBP from multiple donors is helpful, yet will only confer resistance to the diversity of strains present locally (Lower Right) Global pooling from multiple sites will yield passive immunity, and potentially preventative prophylaxis to a greater diversity of viral strains.

***Figure 2*:** (a) Connectivity plots generated from the time course of cumulative (left) and relative (right) for cases (top) and deaths (bottom) (b) Connectogram plots of COVID-19 cases calculated for each month since the initial cases were reported. These connectograms represent the correlations (connections) of the relative COVID case numbers within or across the large-scale communities in the United States according to their geographic position on the continent: the Northeast, Southeast, Southwest, West, and Midwest. Areas on the outermost ring represent the 55 US states and territories (nodes), organized geographically into these six major communities. The outer circle circumscribes five inner circular heatmaps created to display the values of five centrality measures. Toward the center of the circle, the measures are degree centrality, participation coefficient, K-coreness centrality, eigenvector centrality, and PageRank. Values for each measure were mapped to colors, using a scheme that ranged from the minimum (white) to the maximum (fully saturated color) of the data set. Edges or links in the graph represent a temporal correlation that survived a 10% threshold between nodes; red and black connections represent the between-region and within-region COVID case relationships, respectively. Highly connected subgroups or modules are clearly evident in the Northeast and Southeast. Our analysis pipeline enables the reproduction of key figures, accessing the most up-to-date information (link to Github will be shared upon publication).

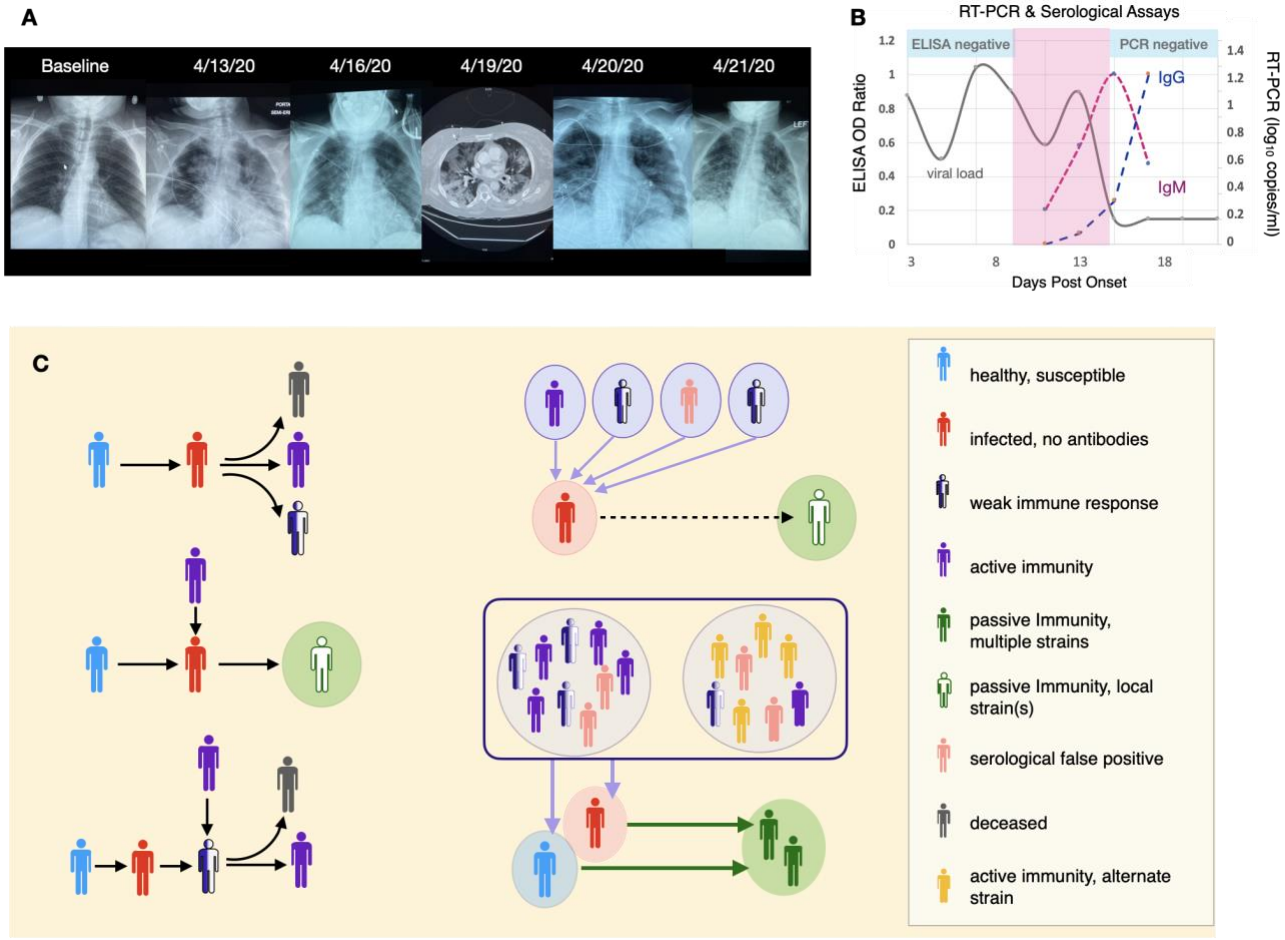
A
Baseline
4/13/20
4/16/20
4/19/20
4/20/20
4/21/20
B
RT-PCR & Serological Assays
ELISA negative
PCR negative
IgG
IgM
viral load
ELISA OD Ratio
RT-PCR (log10 copies/ml)
Days Post Onset
C
healthy, susceptible
infected, no antibodies
weak immune response
active immunity
passive Immunity, multiple strains
passive Immunity, local strain(s)
serological false positive
deceased
active immunity, alternate strain

Figure 2 (a)

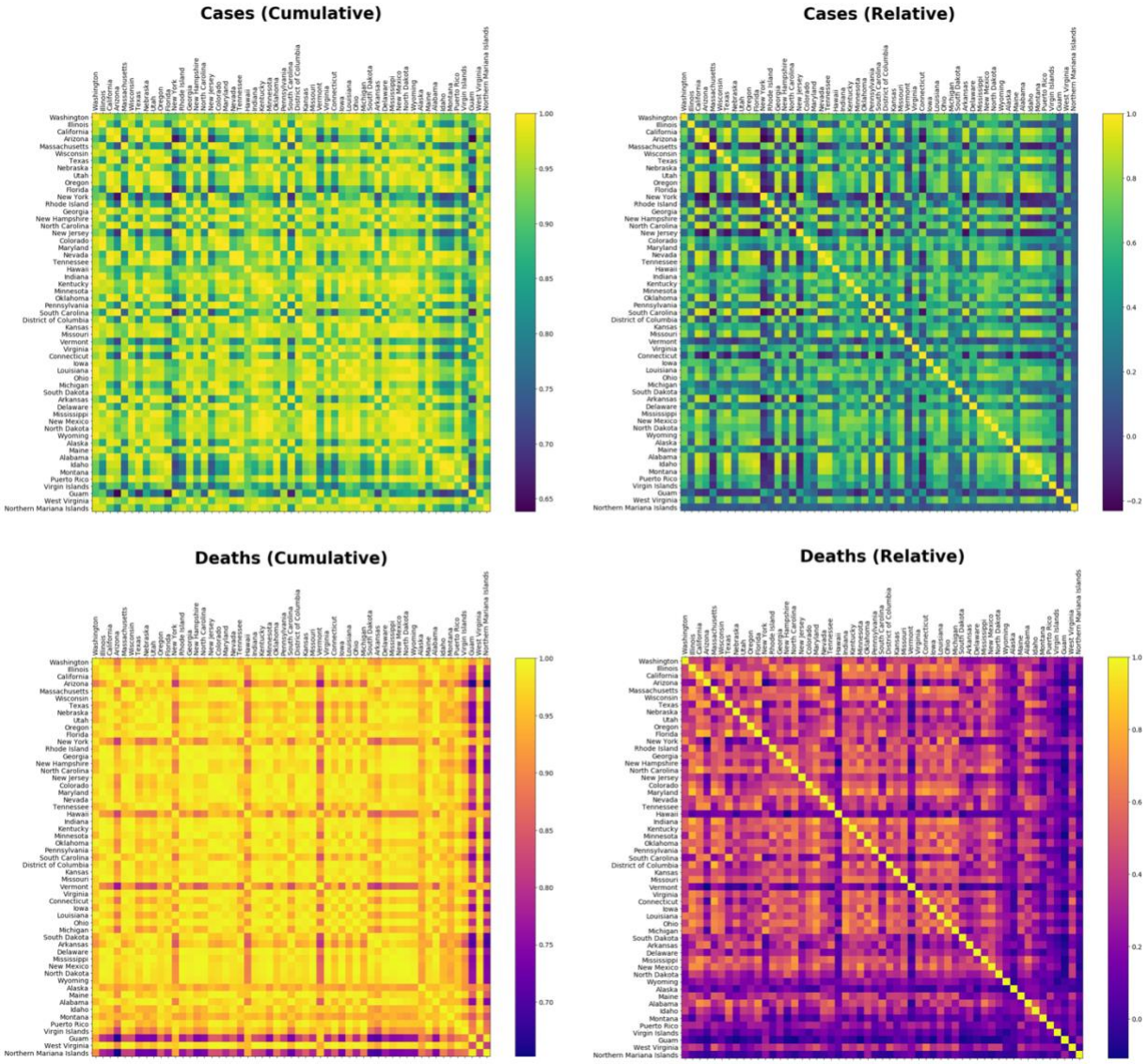
Cases (Cumulative)
Cases (Relative)
Deaths (Cumulative)
Deaths (Relative)

Figure 2(b)

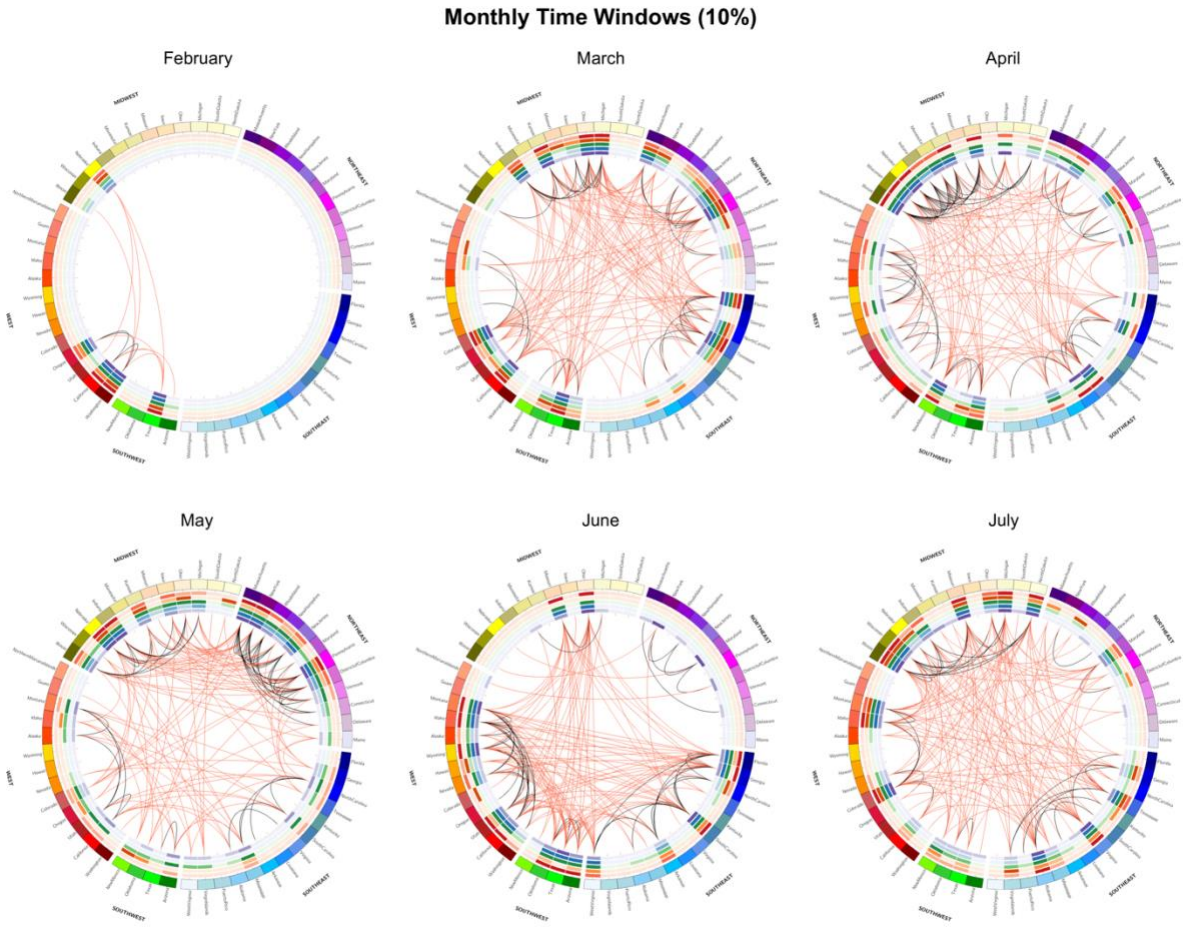

Supplementary methods

Connectivity construction

To perform complex network analysis, we first generated connectivity graphs comprised of nodes (US states and territories) connected by links (the Pearson's correlation coefficient between each pair of nodes), using open source data updated regularly by the New York Times (https://github.com/nytimes/covid-19-data). We constructed a symmetrical correlation matrix with a size of 55×55 for both COVID cases and deaths, relatively and cumulatively (Figure 2b). To examine the dynamic changes of COVID spread between the US states and territories, we formed the aforementioned correlation matrices on a monthly basis. To exclude the confounding effects of spurious links, we thresholded the correlation matrices to preserve a ratio of the strongest connections and remove weaker connections. This step is followed by binarizing the thresholded matrices to make the computational complexity and network representation more tractable.

Computation of graph properties

Using binary undirected matrices, we examined the topological properties of correlation network for each month (from February to August 2020) at both global and local levels. Global measures primarily reveal the functional segregation and integration of the brain network including the mean clustering coefficient, average shortest path length, and small-worldness (31, 32, 33). Local properties are calculated for each individual node (US states and territories) separately, reflecting the nodal centrality and density of hubs (either connector or provincial) in the network. In this study, we calculated the most common centrality metrics such as degree, participation coefficient, K-coreness centrality, eigenvector centrality, and PageRank (33).

Global properties: Supplementary figure 1 depicts the variations of computed global measures for COVID case networks across the time (monthly). The clustering coefficient quantifies the extent to which the neighbors of a given node are interconnected. A a higher mean clustering coefficient value indicates the prevalence of strongly interconnected communities. Characteristic path length reflects the global viral transmission of the network by averaging the shortest path length across all pairs. Small-world networks are neither random nor regular, and consisting of a large number of short-range connections alongside a few long-range shortcuts. Mathematically, small-world networks have a high clustering coefficient and short average path length, which makes them superior to other networks in terms of local segregation and global integration (31, 33). A small-worldness higher than 1 reflects the efficiency of the connectivity network (33), indicating a health hazard in COVID spread, for example. Interestingly, the small-worldness of covid transmission appeared to peak in May, coinciding with the reopening of many states, reduced social distancing, and return to domestic travel.

Supplementary Figure 1. Changes of global properties in the correlation network of COVID cases across the time.

Local properties: The monthly connectivity profiles within/between the US regions are visualized in Figure 3 (sparsity level of 0.1) using Circos software (Krzywinski et al., 2009). Areas on the outermost circle represent the 55 US states and territories in six major communities. This outer circle circumscribes five inner circular heatmaps created to display the values of five centrality measures. Toward the center of the circle, the measures are degree centrality, participation coefficient, K-coreness centrality, eigenvector centrality, and PageRank. Values for each measure were mapped to colors, using a scheme that ranged from the minimum to the maximum of the data set. The red and black curves indicate the correlations (connections) of the relative COVID cases between and within communities, respectively (see Figure 2c).

References:

1. E. V. Behring, Ueber das Zustandekommen der Diphtherie-Immunität und der Tetanus-Immunität bei Thieren (2013), doi:10.17192/EB2013.0164.

2. A. Casadevall, M. D. Scharff, Return to the Past: The Case for Antibody-Based Therapies in Infectious Diseases. *Clinical Infectious Diseases*. **21**, 150–161 (1995).

3. P. Zhou, X.-L. Yang, X.-G. Wang, B. Hu, L. Zhang, W. Zhang, H.-R. Si, Y. Zhu, B. Li, C.-L. Huang, H.-D. Chen, J. Chen, Y. Luo, H. Guo, R.-D. Jiang, M.-Q. Liu, Y. Chen, X.-R. Shen, X. Wang, X.-S. Zheng, K. Zhao, Q.-J. Chen, F. Deng, L.-L. Liu, B. Yan, F.-X. Zhan, Y.-Y. Wang, G.-F. Xiao, Z.-L. Shi, A pneumonia outbreak associated with a new coronavirus of probable bat origin. *Nature*. **579**, 270–273 (2020).

4. B. E. Young, S. W. X. Ong, S. Kalimuddin, J. G. Low, S. Y. Tan, J. Loh, O.-T. Ng, K. Marimuthu, L. W. Ang, T. M. Mak, S. K. Lau, D. E. Anderson, K. S. Chan, T. Y. Tan, T. Y. Ng, L. Cui, Z. Said, L. Kurupatham, M. I.-C. Chen, M. Chan, S. Vasoo, L.-F. Wang, B. H. Tan, R. T. P. Lin, V. J. M. Lee, Y.-S. Leo, D. C. Lye, for the Singapore 2019 Novel Coronavirus Outbreak Research Team, Epidemiologic Features and Clinical Course of Patients Infected With SARS-CoV-2 in Singapore. *JAMA*. **323**, 1488 (2020).

5. W. Guan, Z. Ni, Y. Hu, W. Liang, C. Ou, J. He, L. Liu, H. Shan, C. Lei, D. S. C. Hui, B. Du, L. Li, G. Zeng, K.-Y. Yuen, R. Chen, C. Tang, T. Wang, P. Chen, J. Xiang, S. Li, J. Wang, Z. Liang, Y. Peng, L. Wei, Y. Liu, Y. Hu, P. Peng, J. Wang, J. Liu, Z. Chen, G. Li, Z. Zheng, S. Qiu, J. Luo, C. Ye, S. Zhu, N. Zhong, Clinical Characteristics of Coronavirus Disease 2019 in China. *N Engl J Med*. **382**, 1708–1720 (2020).

6. E. de Wit, N. van Doremalen, D. Falzarano, V. J. Munster, SARS and MERS: recent insights into emerging coronaviruses. *Nat Rev Microbiol*. **14**, 523–534 (2016).

7. C. I. Paules, H. D. Marston, A. S. Fauci, Coronavirus Infections—More Than Just the Common Cold. *JAMA*. **323**, 707 (2020).

8. P. K. Douglas, Preparing for pandemic influenza and its aftermath: mental health issues considered. *Int J Emerg Ment Health*. **11**, 137–144 (2009).

9. Y. Zhou, Y. Hou, J. Shen, Y. Huang, W. Martin, F. Cheng, Network-based drug repurposing for novel coronavirus 2019-nCoV/SARS-CoV-2. *Cell Discov*. **6**, 14 (2020).

10. Y. Cheng, R. Wong, Y. O. Y. Soo, W. S. Wong, C. K. Lee, M. H. L. Ng, P. Chan, K. C. Wong, C. B. Leung, G. Cheng, Use of convalescent plasma therapy in SARS patients in Hong Kong. *Eur J Clin Microbiol Infect Dis*. **24**, 44–46 (2005).

11. K. Duan, B. Liu, C. Li, H. Zhang, T. Yu, J. Qu, M. Zhou, L. Chen, S. Meng, Y. Hu, C. Peng, M. Yuan, J. Huang, Z. Wang, J. Yu, X. Gao, D. Wang, X. Yu, L. Li, J. Zhang, X. Wu, B. Li, Y. Xu, W. Chen, Y. Peng, Y. Hu, L. Lin, X. Liu, S. Huang, Z. Zhou, L. Zhang, Y. Wang, Z. Zhang, K. Deng, Z. Xia, Q. Gong, W. Zhang, X. Zheng, Y. Liu, H. Yang, D. Zhou, D. Yu, J. Hou, Z. Shi, S. Chen, Z. Chen, X. Zhang, X. Yang,

Effectiveness of convalescent plasma therapy in severe COVID-19 patients. *Proc Natl Acad Sci USA*. **117**, 9490–9496 (2020).

12. J. Mair-Jenkins, M. Saavedra-Campos, J. K. Baillie, P. Cleary, F.-M. Khaw, W. S. Lim, S. Makki, K. D. Rooney, Convalescent Plasma Study Group, J. S. Nguyen-Van-Tam, C. R. Beck, The Effectiveness of Convalescent Plasma and Hyperimmune Immunoglobulin for the Treatment of Severe Acute Respiratory Infections of Viral Etiology: A Systematic Review and Exploratory Meta-analysis. *J Infect Dis.* **211**, 80–90 (2015).

13. H. Momattin, K. Mohammed, A. Zumla, Z. A. Memish, J. A. Al-Tawfiq, Therapeutic Options for Middle East Respiratory Syndrome Coronavirus (MERS-CoV) – possible lessons from a systematic review of SARS-CoV therapy. *International Journal of Infectious Diseases*. **17**, e792–e798 (2013).

14. R. Srivastava, C. Ramakrishna, E. Cantin, Anti-inflammatory activity of intravenous immunoglobulins protects against West Nile virus encephalitis. *Journal of General Virology*. **96**, 1347–1357 (2015).

15. G. Marano, S. Vaglio, S. Pupella, G. Facco, L. Catalano, G. M. Liumbruno, G. Grazzini, Convalescent plasma: new evidence for an old therapeutic tool? *Blood Transfusion* (2015), doi:10.2450/2015.0131-15.

16. S. Jolles, W. A. C. Sewell, S. A. Misbah, Clinical uses of intravenous immunoglobulin. *Clin Exp Immunol*. **142**, 1–11 (2005).

17. J. H. O. Hoffmann, A. H. Enk, High-Dose Intravenous Immunoglobulin in Skin Autoimmune Disease. *Front. Immunol.* **10**, 1090 (2019).

18. C. Pérez-Cameo, J. Marín-Lahoz, Serosurveys and convalescent plasma in COVID-19. *EClinicalMedicine*, 100370 (2020).

19. J. Kubota, S. Hamano, A. Daida, E. Hiwatari, S. Ikemoto, Y. Hirata, R. Matsuura, D. Hirano, Predictive factors of first dosage intravenous immunoglobulin-related adverse effects in children. *PLoS ONE*. **15**, e0227796 (2020).

20. S. Kivity, U. Katz, N. Daniel, U. Nussinovitch, N. Papageorgiou, Y. Shoenfeld, Evidence for the Use of Intravenous Immunoglobulins—A Review of the Literature. *Clinic Rev Allerg Immunol*. **38**, 201–269 (2010).

21. C. Wang, Z. Liu, Z. Chen, X. Huang, M. Xu, T. He, Z. Zhang, The establishment of reference sequence for SARS-CoV-2 and variation analysis. *J Med Virol*. **92**, 667–674 (2020).

22. L. Chen, L. Zhong, Genomics functional analysis and drug screening of SARS-CoV-2. *Genes & Diseases*, S2352304220300544 (2020).

23. K. G. Andersen, A. Rambaut, W. I. Lipkin, E. C. Holmes, R. F. Garry, The proximal origin of SARS-CoV-2. *Nat Med*. **26**, 450–452 (2020).

24. W. Li, Bats Are Natural Reservoirs of SARS-Like Coronaviruses. *Science*. **310**, 676–679 (2005).

25. D. K. W. Chu, Y. Pan, S. M. S. Cheng, K. P. Y. Hui, P. Krishnan, Y. Liu, D. Y. M. Ng, C. K. C. Wan, P. Yang, Q. Wang, M. Peiris, L. L. M. Poon, Molecular Diagnosis of a Novel Coronavirus (2019-nCoV) Causing an Outbreak of Pneumonia. *Clinical Chemistry*. **66**, 549–555 (2020).

26. B. Korber, W. Fischer, S. Gnanakaran, H. Yoon, J. Theiler, W. Abfalterer, B. Foley, E. Giorgi, T. Bhattacharya, M. Parker, D. Partridge, C. Evans, T. Freeman, T. de Silva, on behalf of the Sheffield COVID-19 Genomics Group, C. LaBranche, D. Montefiori, "Spike mutation pipeline reveals the emergence of a more transmissible form of SARS-CoV-2" (preprint, Evolutionary Biology, 2020), , doi:10.1101/2020.04.29.069054.

27. X. Tang, C. Wu, X. Li, Y. Song, X. Yao, X. Wu, Y. Duan, H. Zhang, Y. Wang, Z. Qian, J. Cui, J. Lu, On the origin and continuing evolution of SARS-CoV-2. *National Science Review*, nwaa036 (2020).

28. R. L. Graham, R. S. Baric, Recombination, Reservoirs, and the Modular Spike: Mechanisms of Coronavirus Cross-Species Transmission. *JVI*. **84**, 3134–3146 (2010).

29. J. K. Taubenberger, J. C. Kash, D. M. Morens, The 1918 influenza pandemic: 100 years of questions answered and unanswered. *Sci. Transl. Med.* **11**, eaau5485 (2019).

30. D. Wrapp, N. Wang, K. S. Corbett, J. A. Goldsmith, C.-L. Hsieh, O. Abiona, B. S. Graham, J. S. McLellan, Cryo-EM structure of the 2019-nCoV spike in the prefusion conformation. *Science*. **367**, 1260–1263 (2020).

31. D. S. Bassett, E. Bullmore, Small-World Brain Networks. *Neuroscientist*. **12**, 512–523 (2006).

32. F. V. Farahani, M. Fafrowicz, W. Karwowski, P. K. Douglas, A. Domagalik, E. Beldzik, H. Oginska, T. Marek, Effects of Chronic Sleep Restriction on the Brain Functional Network, as Revealed by Graph Theory. *Front. Neurosci.* **13**, 1087 (2019).

33. M. Rubinov, O. Sporns, Complex network measures of brain connectivity: Uses and interpretations. *NeuroImage*. **52**, 1059–1069 (2010).

34. R. Gomulkiewicz, J. N. Thompson, R. D. Holt, S. L. Nuismer, M. E. Hochberg, Hot Spots, Cold Spots, and the Geographic Mosaic Theory of Coevolution. *The American Naturalist*. **156**, 156–174 (2000).

35. D. G. Streicker, P. Lemey, A. Velasco-Villa, C. E. Rupprecht, Rates of Viral Evolution Are Linked to Host Geography in Bat Rabies. *PLoS Pathog*. **8**, e1002720 (2012).

36. X. Yu, T. Tsibane, P. A. McGraw, F. S. House, C. J. Keefer, M. D. Hicar, T. M. Tumpey, C. Pappas, L. A. Perrone, O. Martinez, J. Stevens, I. A. Wilson, P. V. Aguilar, E. L. Altschuler, C. F. Basler, J. E. C. Jr, Neutralizing antibodies derived from the B cells of 1918 influenza pandemic survivors. *Nature*. **455**, 532–536 (2008).

37. A. S. Gonzalez-Reiche, M. M. Hernandez, M. Sullivan, B. Ciferri, H. Alshammary, A. Obla, S. Fabre, G. Kleiner, J. Polanco, Z. Khan, B. Alburquerque, A. van de Guchte, J. Dutta, N. Francoeur, B. S. Melo, I. Oussenko, G. Deikus, J. Soto, S. H. Sridhar, Y.-C. Wang, K. Twyman, A. Kasarskis, D. R. Altman, M. Smith, R. Sebra, J. Aberg, F. Krammer, A. Garcia-Sarstre, M. Luksza, G. Patel, A. Paniz-Mondolfi, M. Gitman, E. M. Sordillo, V. Simon, H. van Bakel, "Introductions and early spread of

SARS-CoV-2 in the New York City area" (preprint, Infectious Diseases (except HIV/AIDS), 2020), , doi:10.1101/2020.04.08.20056929.

38. N. Kriegeskorte, P. K. Douglas, Cognitive computational neuroscience. *Nat Neurosci*. **21**, 1148–1160 (2018).

39. Y. Pan, D. Zhang, P. Yang, L. L. M. Poon, Q. Wang, Viral load of SARS-CoV-2 in clinical samples. *The Lancet Infectious Diseases*. **20**, 411–412 (2020).